International Journal of Steel Structures
https://doi.org/10.1007/s13296-024-00874-z

Online ISSN 2093-6311
Print ISSN 1598-2351

Experimental Investigation of the Effect of Welding Parameters on Material Properties of SS 316L Stainless Steel Welded Joints

Rameshwar V. Chavan[1,2] · **Anirban C. Mitra**[3]

Received: 28 August 2023 / Accepted: 14 July 2024

Abstract
A wire is fed into the MIG welding gun, where it sparks and melts to form the weld. It is frequently semi-automated or automatic. TIG welding uses a non-consumable electrode and a separate filler material to combine metals with long rods. TIG and MIG welding are commonly used in industries like pressure vessels, economizers, and Air preheater manufacturing. Combining these processes to optimize benefits and reduce drawbacks is explored. High-thickness welding, found in nuclear reactor core manufacturing, often uses submerged arc welding, but costly. TIG–MIG welding is proposed for 10–40 mm SS316L plates, reducing costs with maintained strength. Design of Experiment is used to vary control parameters. Present article research on SS316L up to 12 mm thick revealed that the following settings would yield the best tensile strength and hardness: 170 A for the welding current, 3 mm for the filler wire diameter, and 14 L/min for the gas flow rate. Values from the experiment and prediction were nearly identical.

Keywords High thickness · SS316L · Heat affected zone (HAZ) · TIG–MIG · Ultimate tensile strength (UTS) · Micro hardness (MH) · Design of experiment (DoE)

1 Introduction

Tungsten inert gas–metal inert gas (TIG–MIG) hybrid welding combines the benefits of both metal inert gas (MIG) and tungsten inert gas (TIG) welding. It is a successful strategy to increase welding productivity and quality due to the advantages of the two welding techniques (Cui et al., 2023). Linger et al. found the experimental analysis method was used, and L16 was used to conduct the experiment on 304L stainless steel. The root gap, welding current, gas flow rate, arc length, and welding travel speed were the welding parameters that were chosen. The mechanical characteristics of the weld joint underwent tests for Rockwell hardness, tensile strength, and bending strength, based on the Taguchi method with a grey base (Linger & Bogale, 2023). Ghumman et al. found that arc current is the key factor in optimizing responses. For lowest surface roughness, they recommend current 125 A, voltage 18 V, and gas flow rate 12 L/min. Maximum hardness was achieved with current 125 A, voltage 20 V, and gas flow rate 9 L/min. The highest tensile strength resulted from a combination of current 100 A, voltage 18 V, and gas flow rate 6 L/min (Ghumman et al., 2022). Abima et al. discussed the microstructure of the TIG–MIG joint revealed an abundance of acicular ferrite with cementite on the ferrite grain boundaries. Martensite phases diffracted at higher intensity peaks in the TIG weld, while iron phases diffracted at high-intensity peaks in the MIG weld. Finally, the TIG–MIG welded joint revealed only iron phases, accounting for its lowest hardness value when compared to standalone MIG and TIG joints (Abima, 2022). Azevedo and de Resende studied by setting the TIG current, TIG torch angle, and MIG/MAG torch angle to their maximum values and the distance between the electrodes to their minimum values, a larger fusion zone area and penetration are achieved. When the TIG current and MIG/MAG torch angle are set to their lowest values and the distance between the electrodes and TIG torch angle

✉ Rameshwar V. Chavan
rameshwarchavan@dietms.org; rvchavan2022@gmail.com

Anirban C. Mitra
amitra@mescoepune.org

[1] Mechanical Engineering Department, AISSMS College of Engineering, Pune 411001, India

[2] Mechanical Engineering Department, DIEMS Aurangabad, Chhatrapati Sambhajinagar 431005, India

[3] Mechanical Engineering Department, M.E.S. College of Engineering, Pune 411001, India

Published online: 22 July 2024

are set to their highest values, respectively, a wider bead is produced (Azevedo & Resende, 2021). Abdul Kadir et al. studied industries that require high-quality welding, such as the beverage, nuclear power plant, industrial, and petrochemical industries, combined heat and power plants, and the offshore industry, tungsten inert gas (TIG) and metal inert gas (MIG) welding is frequently used. Additionally, TIG MIG welding is used in the fields of aerospace, fine art, automotive manufacturing, food manufacturing, and building and construction (Abdul Kadir et al., 2021). Somani and Lalwani found the mechanical and metallurgical characteristics of austenitic stainless steel SA 240 Gr. 304 plate samples welded using the TIG-MG hybrid welding process were examined by Somani and Lalwani (2020). Further revealed that using Design Expert software, an attempt is made to statistically analyze and improve control parameters. Based on significant control parameters, a statistical model is created (Somani & Lalwani, 2019). Ogundimu et al. further investigated all of the welded joints and demonstrated excellent joint strength, demonstrating that 6 mm thick plates can be successfully welded using TIG–MIG hybrid welding of type 304 austenitic stainless steel. It was discovered that as the heat input increases, the welding joint's efficiency decreases. In all three joints' heat-affected zones, there is noticeable grain coarsening, which gets smaller as the heat input gets lower. Compared to the other participating samples, sample A3 has a larger dendrite formation in the fusion zone (Ogundimu et al., 2019). Huang et al. pointed out that the assisted TIG arc's preheating and steady arc functions enable it to address sidewall incomplete penetration in NG-GMAW. MIG welding wire that has melted flows into the TIG molten pool, resulting in wider welds and better sidewall penetration (Huang et al., 2019). Zong et al. suggested that to describe the arc stability, the waveform of the welding current–voltage was examined. Even at TIG currents as low as 50 A when the TIG arc was leading, the hybrid arc was more stable than traditional MIG welding. However, when the TIG arc was trailing, the TIG current needed to be greater than 100 A to prevent spatters. To explain the heat and force, the arc shape and droplet transfer were studied (Zong et al., 2019). Balaram Naik and Chennakeshava Reddy indicated that to increase the weld's tensile strength, hardness, and depth by adjusting variables like electrode diameter, gas flow rate, current, time, and speed. Results are analyzed using the Mat Lab software, which demonstrates that using a neural network along with the Taguchi method, ANOVA, and other techniques is an efficient way to improve the weld quality of the material (Balaram Naik & Chennakeshava Reddy, 2018). Chen et al. further investigated the microstructure analysis and the HAZ of a TIG–MIG hybrid weld joint narrowed while no obvious grain coarsening was evident in the weld zone, suggesting that prominent dendrite formation occurred at higher welding speeds (Chen et al., 2017). Samir Khan et al. observed the welding of 10 mm thick 304L stainless steel plates using a combined TIG–MIG process. They found that increasing the gas flow rate led to a decrease in weld bead hardness, although it also caused slight bead width expansion. High gas flow rates induced turbulence, negatively affecting weld quality. Optimal welding voltage and current were around 24 V and 200 A, respectively, for achieving the best hardness and bead width values. A gas flow rate between 15 and 17 l/min was deemed suitable for the process (Samir Khan et al., 2018). Schneider et al. observed the type of shielding gas used (MIG/MAG), the voltage, the wire feed rate, and the welding speed were the variables that had a significant impact on penetration. Shielding gas type (MIG/MAG), voltage (MIG/MAG), electric current intensity (TIG), and welding speed all had a sizable impact on the HAZ (Schneider et al., 2017).

In the current study, the effects of the TIG MIG welding parameters of current, filler rod diameter and gas flow rate, hardness, and ultimate tensile strength properties were examined. Material SS 316L stainless steel plates used and experiments were carried out. Filler material made of SS 316L is used. Experimentation was done using Taguchi L4 orthogonal design array. With the aid of Taguchi analysis, the results were examined, and use of analysis of variance. The scope of the work involves a systematic investigation aimed at understanding how different welding parameters affect the material properties of SS 316L stainless steel welded joints, with the ultimate goal of improving the quality and reliability of welded structures in various engineering applications.

2 Methodlogy

2.1 Experimental Set Up

Figures 1 and 2 shows the TIG and MIG experimental machine setup and Table 1 represents the TIG MIG Machine Specification. All the experiments were conducted at Shani Krupa Enterprises, MIDC Waluj, Chhatrapati Sambhajinagar, M.S, India.

2.2 Selection of Material

2.2.1 SS 316L

The stainless-steel SS 316L plate with a thickness of 12 mm was used for TIG MIG welding. The 12 mm thickness for the SS 316L stainless steel plate was chosen due to a literature gap focusing on higher thicknesses. This study aims to fill this void by investigating material strength and post-welding behavior, contributing to underexplored research in the field. It serves as a base metal.

Fig. 1 TIG machine

Fig. 2 MIG machine

SS 3316L is an austenitic metallic alloy of stainless steel with nickel and molybdenum that makes it corrosion resistant and it has superior strength and toughness. Figure 3 shows the sample of material and Table 2 shows the chemical composition of the SS 316L.

2.2.2 Sample Preparation

2.2.2.1 Geometry Preparation See Fig. 4.

Material: SS316L.

Dimensions: 50 mm length * 50 mm wide * 12 mm thickness.

Fillet weld joint.

2.3 Experimental Design

It is common practice to assess the primary impacts plot or the signal to noise ratio as a way to properly comprehend how input variables like welding current, Filler wire size, and gas flow rate affect the ultimate tensile strength of the resultant product. Based on these considerations, the choice of welding current, Filler wire size, and gas flow rate seems appropriate for evaluating their effects on the material properties of SS 316L stainless steel welded joints. These parameters encompass key aspects of the welding process and are likely to provide valuable insights into optimizing the welding procedure for achieving desired material properties and weld quality.

This has been done using the Design of Experiment software Minitab 19. It was decided to investigate the ultimate tensile strength and micro hardness of the welded samples. The ultimate tensile strength was studied using ANOVA to determine the impact of each parameter, and a linear regression model was developed to forecast the values of the ultimate tensile strength. The L4 orthogonal array is displayed in Table 3 along with UTS measurements for runs 1 through 4. It also displays the S/N ratio for each of the four experiments.

Minitab 19 software is used to calculate the S/N ratio data. The S/N ratio throughout all studies shows very little change, as can be observed.

2.3.1 UTS's Primary Effects

Figure 5 represents the primary impacts graph based on S/N ratios.

Table 1 TIG_MIG machine specification

Model	TIG	MIG
Manufactured	China	China
Ampere	5–250 A	50–250 A
Weld able Materials	Aluminium, mild steel, copper, stainless steel, titanium, and nickel alloy	Carbon steel, stainless steel, mild steel, aluminum and nickel alloy
Input voltage	220–240 v	AC 415 V
Welder dimensions	14 in × 8 in × 16 in	14.5 × 6 × 9
Weight	35 lbs	44 lbs

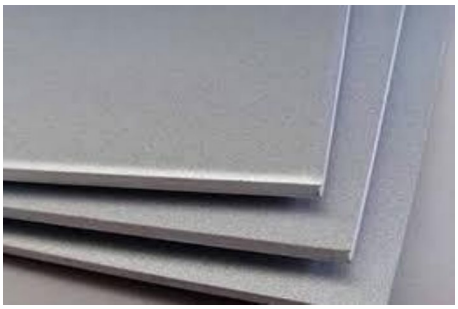

Fig. 3 SS 316L

The MINITAB software was used to calculate a higher SN ratio with better characteristics for the experimental tests, and it was found that the response graph's lowest values corresponded to the best material removal rate. Welding current 150 A (level 2), filler wire diameter 3.0 mm (level 2), and gas flow rate 14 l/min (level 2) were the ideal input parameters. The control factors' effects on the SS316L material are depicted graphically in the graph. With the least amount of variation, the highest ratio configuration of the process parameters always yields the best quality. The relationship changed as indicated by the controlling factor configuration changed from a single level to another as seen by the graph.

2.3.2 ANOVA Findings

ANOVA, often known as Fisher's ratio (F), calculates the correlation between the primary parameter's variance and the error's variance. The parameter's F test value and the average F table value are compared at the *P* significant level, one can determine whether the parameter significantly affects the quality characteristic Cutting parameter significance is determined by whether the F test value exceeds the *P* test. The models' applicability is assessed using analysis of variance (ANOVA).

It is a statistical method used to test the null hypothesis in planned experiments that look at numerous variables at once. The Fisher test (F test) is used to quickly analyze the experiment's variances using ANOVA. The results of the ANOVA analysis are displayed in an ANOVA table. It is possible to see from an ANOVA analysis that in each of the three parametric sources, *P* is less than 0.05. It is evident that the CRCA material is influenced by the filler wire diameter, welding current, and gas flow rate of the material. The cumulative ANOVA's final column showed each factor's

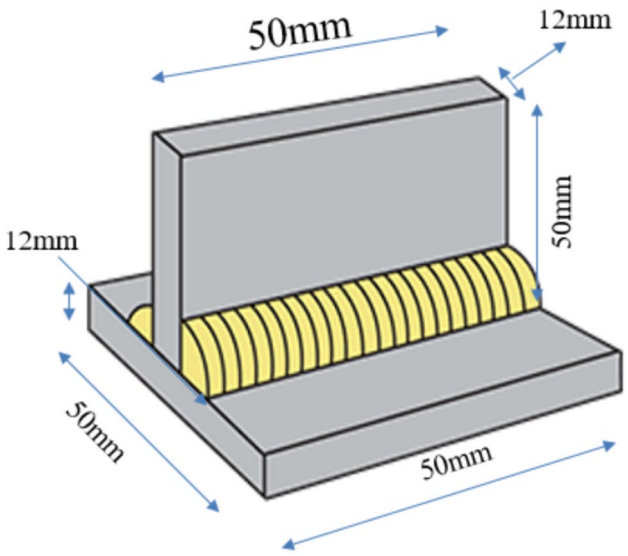

Fig. 4 T joint with 50 mm length * 50 mm wide * 12 mm thickness

Table 3 The response characteristics of an orthogonal L4 array

Experiments	Inputs			Output	
Trial numbers	Welding current	Filler wire diameter	Gas flow rate	UTS	S/N ratio
1	150	2.6	10	620	55.7066
2	150	3.0	14	673	56.2449
3	170	2.6	14	609	56.4955
4	170	3.0	10	641	56.1372

share of the total variance, showing how strongly it affected the outcome. The analysis of variance's results are shown in Table 4.

The Table 4 shows that the welding current (46.95%), the filler wire diameter (13.15%) and gas flow rate (34.90%) significantly affect the UTS.

2.3.3 Regression Model Development for UTS

Minitab software has been used to create the regression model the moisture content values for each level of study parameters were estimated based on the measured values of the variables included in the regression equation. The correlation between the predicted and experimental moisture content values can also be seen graphically.

Table 2 SS316L steel's chemical content

C	Si	Mn	S	Cr	Ni	N	Mo	Fe
0.03	1.0	2.00	0.015	16.50	10.00	0.10	2.00	Balance

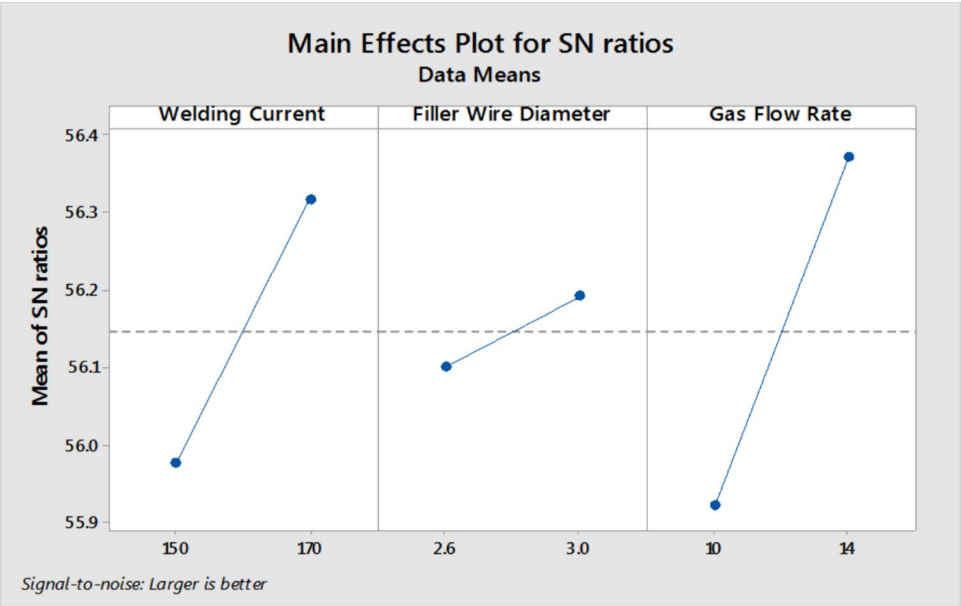

Fig. 5 S/N ratio main effects plot

Table 4 ANOVA results

Source	DF	Adj SS	Adj MS	F value	*P* value	% contribution
Welding process current (A)	1	0.24334	0.12167	9.41	0.013	46.95
Filler wire diameter (B)	1	0.06819	0.03409	2.63	0.047	13.15
Gas flow rate (C)	1	0.18091	0.09045	6.97	0.035	34.90
Residual error	1	0.02584	0.01292			4.98
Total	4	0.51828				

2.3.4 Regression Equation

$$\text{UTS} = 301.0 + 1.250\ \text{Welding Current (A)} + 15.00\ \text{Filler Wire Diameter } (B) + 8.250\ \text{Gas Flow Rate(C)}$$

Table 5 compares experimentally determined and anticipated moisture content using a derived mathematical equation.

The UTS values predicted using the regression equation and the experimental values of each encounter were found to differ by less than 10%. As a result, we can conclude that the regression equation was accurate.

2.3.5 Confirmation Experiment Results

The moisture content value obtained from the confirmation experiment is compared to the value predicted by the created regression model in Table 5. Table 6 shows the results of the confirmation experiment.

The Taguchi method's recommended parameter settings are used to conduct a confirmation experiment and the resulting UTS value was compared to the value predicted by the regression model while keeping the parameter values constant. It is clear that the experimental result and the projected outcome differ by 1.18%. This implies a connection between the experimental value and the estimated value.

Table 5 Values of UTS that have been predicted and tested

Sr. No.	Experimental value	Predicted value	Error %
1	620	610	1.63
2	673	649	3.69
3	609	668	8.88
4	641	652	1.68

Table 6 Results of the confirmation experiment

Parameter	Predicted value	Experimental value	Error %
Ultimate tensile strength	674	682	1.18

Table 7 Micro hardness experiment result

Parameter	TIG (Hv)	MIG (Hv)
Base metal	310–315	310–315
Heat affected zone (HAZ)	320–325	325–330
Weld area	330–337	325–342

2.4 Results of the Micro Hardness Experiment

Table 7 represents the microhardness experimental results for TIG and MIG welding.

3 Results and Discussion

Based on above DOE experimentation Fig. 5 represents the primary impacts graph based on S/N ratios and summarized as welding current 150 A (level 2), filler wire diameter 3.0 mm (level 2), and gas flow rate 14 l/min (level 2) were the ideal input parameters whereas ANOVA results shows that the welding current (46.95%), the filler wire diameter (13.15%) and gas flow rate (34.90%) significantly affect the UTS. Table 5 compares experimentally determined and anticipated moisture content using a derived mathematical equation. Table 6 represents the ultimate tensile strength value was compared to the value predicted by the regression model while keeping the parameter values constant. It is clear that the experimental result and the projected outcome differ by 1.18%. This implies a connection between the experimental value and the estimated value.

4 Conclusions

To be able to thoroughly investigate the effects of welding on stainless steel 316L material, this study includes observations about the UTS over the Austenitic stainless steel 316L made using a TIG–MIG welding machine for various input parameters. Throughout the experiment, obtained the following results.

- Based on a combination of the welding parameters and levels, welding current 170 A was found to be the best solution for UTS, filler wire diameter 3 mm and Gas flow rate 14 l/min. The Welding current more significant parameters than filler wire diameter and gas flow rate.
- Micro hardness for MIG on the base metal, heat affected zone, and weld area is 310 Hv, 320 Hv, 330 Hv, respectively, while TIG's values are 310 Hz, 325 Hv, and 335 Hv, respectively.
- Maximum hardness was attained when current 170 A, filler wire diameter 3 mm, and gas flow rate 14 l/min were combined parametrically
- The results of the ANOVA show that welding current has a significant impact on the final tensile strength. Welding current, filler wire diameter, and gas flow rate all contribute different amounts respectively, 46.95%, 13.15%, and 34.90% to the quality characteristics of Ultimate tensile strength.
- Taguchi methods are used to determine the ideal cutting parameters, which match experimental values with the fewest errors possible at 1.18%.
- It is possible to estimate experimental results of ultimate tensile strength for any set of TIG MIG parameters using the developed mathematical models.

Acknowledgements The authors would like to gratefully acknowledge the facilities provided by the Deogiri Institute of Engineering and management studies, Chhatrapati Sambhajinagar, AISSMS College of Engineering, Pune and M.E.S. College of Engineering, Pune

Funding The authors declare there is no financial support from anyone for this work.

Data availability Data will be made available on request.

Declarations

Conflict of interest All authors declare that they have no conflicts of interest.

References

Abdul Kadir, M. H., Asmelash, M., & Azhari, A. (2021). Investigation on welding distortion in stainless steel sheet using gas tungsten arc welding process. *Materials Today: Proceedings, 46*, 1674–1679. https://doi.org/10.1016/j.matpr.2020.07.264

Abima, C. S., Akinlabi, S. A., et al. (2022). Comparative study between TIG–MIG Hybrid, TIG and MIG welding of 1008 steel joints for enhanced structural integrity. *Scientific African*. https://doi.org/10.1016/j.sciaf.2022.e01329

Azevedo, S. C., & de Resende, A. A. (2021). Effect of angle, distance between electrodes and TIG current on the weld bead geometry in TIG–MIG/MAG welding process. *The International Journal of Advanced Manufacturing Technology, 114*(5–6), 1505–1515. https://doi.org/10.1007/s00170-021-07004-7

BalaramNaik, A., & Chennakeshava Reddy, A. (2018). Optimization of tensile strength in TIG welding using the Taguchi method and analysis of variance (ANOVA). *Thermal Science and Engineering Progress, 8*, 327–339. https://doi.org/10.1016/j.tsep.2018.08.005

Chen, J., Zong, R., Wu, C., Padhy, G. K., & Hu, Q. (2017). Influence of low current auxiliary TIG arc on high speed TIG–MIG hybrid welding. *Journal of Materials Processing Technology, 243*, 131–142. https://doi.org/10.1016/j.jmatprotec.2016.12.012

Cui, X., Chen, J., Xia, C., Han, X., Su, H., & Wu, C. (2023). The mechanism study of TIG–MIG hybrid welding process based on simulation. *Vacuum, 215*, 112341. https://doi.org/10.1016/j.vacuum.2023.112341

Ghumman, K. Z., Ali, S., Din, E. U., Mubashar, A., Khan, N. B., & Ahmed, S. W. (2022). Experimental investigation of effect of welding parameters on surface roughness, micro-hardness and tensile strength of AISI 316L stainless steel welded joints using 308L filler material by TIG welding. *Journal of Materials Research and Technology, 21*, 220–236. https://doi.org/10.1016/j.jmrt.2022.09.016

Huang, J., Chen, H., He, J., Yu, S., Pan, W., & Fan, D. (2019). Narrow gap applications of swing TIG–MIG hybrid weldings. *Journal of Materials Processing Technology, 271*, 609–614. https://doi.org/10.1016/j.jmatprotec.2019.04.043

Linger, M. A., & Bogale, T. M. (2023). Parameters optimization of tungsten inert gas welding process on 304L stainless steel using grey based Taguchi method. *Engineering Research Express, 5*(1), 015013. https://doi.org/10.1088/2631-8695/acb526

Ogundimu, E. O., Akinlabi, E. T., & Erinosho, M. F. (2019). An experimental study on the effect of heat input on the weld efficiency of TIG–MIG hybrid welding of type 304 austenitic stainless steel. *Journal of Physics: Conference Series, 1378*(2), 022075. https://doi.org/10.1088/1742-6596/1378/2/022075

Samir Khan, M., Kumar, V., Mandal, P., & Chandra Mondal, S. (2018). Experimental investigation of combined TIG–MIG welding for 304 stainless steel plates. *IOP Conference Series: Materials Science and Engineering, 377*, 012067. https://doi.org/10.1088/1757-899x/377/1/012067

Schneider, C., Lisboa, C., Silva, R., & Lermen, R. (2017). Optimizing the parameters of TIG–MIG/MAG hybrid welding on the geometry of bead welding using the Taguchi method. *Journal of Manufacturing and Materials Processing, 1*(2), 14. https://doi.org/10.3390/jmmp1020014

Somani, C. A., & Lalwani, D. (2019). Experimental investigation of TIG–MIG hybrid welding process on austenitic stainless steel. *Materials Today: Proceedings, 18*, 4826–4834. https://doi.org/10.1016/j.matpr.2019.07.472

Somani, C. A., & Lalwani, D. (2020). Experimental study of some mechanical and metallurgical properties of TIG–MIG hybrid welded austenitic stainless steel plates. *Materials Today: Proceedings, 26*, 644–648. https://doi.org/10.1016/j.matpr.2019.12.253

Zong, R., Chen, J., & Wu, C. (2019). A comparison of TIG–MIG hybrid welding with conventional MIG welding in the behaviors of arc, droplet and weld pool. *Journal of Materials Processing Technology, 270*, 345–355. https://doi.org/10.1016/j.jmatprotec.2019.03.003